Applicability of continuum mechanics to pressure drop in small orifices

Febe Kusmanto
Department of Chemical Engineering, University of Washington, Seattle, Washington 98195-1750

Elissa L. Jacobsen
Department of Chemistry, University of Washington, Seattle, Washington 98195-1750

Bruce A. Finlayson[a)]
Department of Chemical Engineering, University of Washington, P.O. Box 351750, Seattle, Washington 98195-1750

(Received 8 March 2004; accepted 9 August 2004; published online 6 October 2004)

Pressure drop in small orifices (8–109 μm) is examined by comparing the experimental data of Hasegawa, Suganuma, and Watanabe [Phys. Fluids **9**, 1 (1997)] with theoretical and numerical solutions of the Navier–Stokes equations in order to test the claim by Hasegawa, Suganuma, and Watanabe that the data could not be explained by traditional continuum mechanics. The Reynolds number varies from zero (for the theoretical solution to Stokes flow) to 1000. The ratio of the orifice thickness to its diameter varies from 0.092 to 1.14. The primary increase in pressure drop is shown to be due to the effect of a finite thickness of the orifice, and this effect is predicted for Stokes flow by the theory of Dagan, Weinbaum, and Pfeffer [J. Fluid Mech. **115**, 505 (1982)]. Numerical results presented here agree with Dagan, Weinbaum, and Pfeffer at Reynolds numbers below 10 and with the experimental data of Hasegawa, Suganuma, and Watanabe for low and intermediate Reynolds numbers. Most of the data can be predicted using traditional continuum mechanics. © *2004 American Institute of Physics*. [DOI: 10.1063/1.1800051]

I. INTRODUCTION

In their review article, Ho and Tai[1] point out that surface forces can become as important as body forces in determining flow characteristics in small devices ($\approx$10–100 μm). Since surface forces usually scale as size squared and volume forces scale as size cubed, as the size decreases, the relative importance of surface forces increases. This fact is especially important in micromachines, but it is also relevant to microfluidics. The surface forces are van der Waals forces (applicable to all materials), electrostatic forces (especially relevant to ionic fluids), and steric forces (especially relevant to polymers and complex molecules). Due to the increased importance of microfluidics, it is important to know whether traditional continuum mechanics is still valid in these small devices, or if a new theoretical framework is necessary.

Hasegawa, Suganuma, and Watanabe[2] published an extensive set of experiments of the pressure drop for flow through small orifices in capillaries. The orifice diameter ranged from 8.8 to 1024 μm. They concluded that there are unusual, unexplained effects in the smallest devices. This conclusion and the paper of Hasegawa, Suganuma, and Watanabe[2] have been quoted by several recent papers as the authors explain possible discrepancies in their own data in micrometer scale devices. Gijsbertsen-Abrahamse, van der Padt, and Boom[3] use it to explain their experiments in membrane emulsification. Hsiai *et al.*[4] use it to explain their experiments in particle filters. Janssens-Maenhout and Schulenberg[5] invoke the paper to describe the importance of contact angle measurements. Yao and Kim[6] indicate that the viscosity of a polymer measured in a capillary flow experiment might be too high due to similar effects if the capillary size is small since they predict a higher viscosity in a 1 μm thick wall layer. Chen[7,8] refer to the paper of Hasegawa, Suganuma, and Watanabe as showing that nonlinear pressure distributions cannot be adequately explained by conventional theories. Thus, it is important to demonstrate that traditional continuum mechanics can indeed explain most of the data of Hasegawa, Suganuma, and Watanabe.

The present paper shows that for liquids the effects can be, and have been, explained by traditional continuum mechanics. In particular, the theoretical Stokes solution due to Dagan, Weinbaum, and Pfeffer[9] are shown to fit the data of Hasegawa, Suganuma, and Watanabe[2] at Reynolds numbers below 10 for all thickness to diameter (L/D) ratios. The experiments conducted in pipes over 80 years ago by Bond[10,11] also agree with Hasegawa, Suganuma, and Watanabe[2] and Dagan, Weinbaum, and Pfeffer[9] at Reynolds numbers below 10. Numerical solutions are presented here for intermediate Reynolds numbers (1–300) to show that traditional continuum mechanics can predict nearly all the data of Hasegawa, Suganuma, and Watanabe[2] as the Reynolds number is increased as well. Additional complications are important for gases (possible slip and heating effects in compressible fluids), but only liquids are treated here. First, we examine prior work for the Stokes problem and then present known correlations and numerical results for intermediate Reynolds numbers.

[a)]Electronic mail: finlayson@cheme.washington.edu

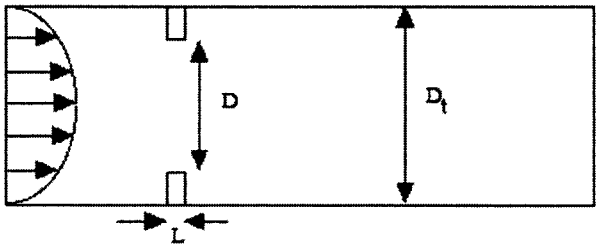

FIG. 1. Geometry of orifice.

II. PRIOR WORK AT LOW REYNOLDS NUMBERS

Hasegawa, Suganuma, and Watanabe[2] presented data for the pressure drop as a function of Reynolds number. The pressure coefficient

$$K \equiv \frac{2\Delta p}{\rho \langle v \rangle^2} \tag{1}$$

was plotted versus Reynolds number

$$\mathrm{Re} \equiv \frac{\rho \langle v \rangle D}{\mu}, \tag{2}$$

where Δp is the pressure drop due to the orifice (above that for fully developed flow in the capillary), ρ is the density, μ is the viscosity, $\langle v \rangle$ is the average velocity through the orifice, and D is the diameter of the orifice. Figure 1 shows the geometry of the orifice, where L is the orifice thickness, D_t is the capillary diameter, and D is defined above, and typical data are shown in Fig. 2. Orifice diameters ranged from 1024 down to 8.8 μm. The thickness of the orifice, L, was varied as well, ranging from 10 to 52 μm. This led to ranges of L/D from 0.051 to 1.14. All data for orifice diameters above 100 μm followed the same line, the line shown in Fig. 2 for $L/D=0.092$. Data for smaller diameter orifices followed distinct curves for each L/D. Hasegawa, Suganuma, and

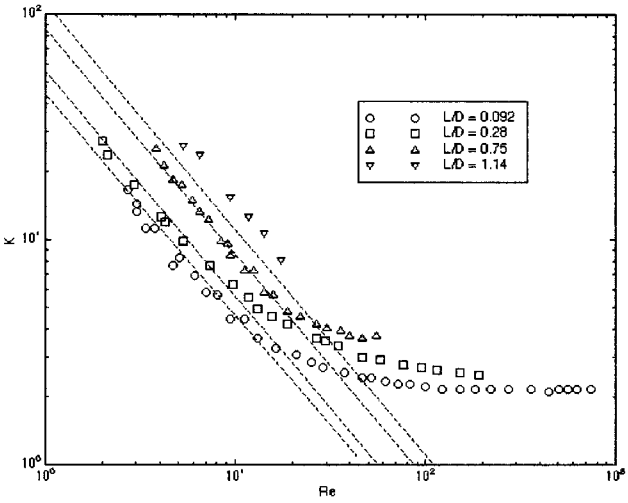

FIG. 2. Pressure coefficient, Eq. (1), as a function of Reynolds number. Points are experimental data of Hasegawa, Suganuma, and Watanabe (Ref. 2). Dotted lines are analytical solutions to Stokes flow [Dagan, Weinbaum, and Pfeffer (Ref. 9)] which are indistinguishable from the data of Bond (Ref. 10).

Watanabe[2] did numerical analysis including orifices with different thicknesses and claimed that they saw no effect of L/D: all results were on the same curve of pressure coefficient versus Reynolds number (following the bottom set of data for $L/D=0.092$ in Fig. 2). To try to explain their data, they investigated the effect of different metal surfaces for the orifice and found no difference. They added a burr on the edge of the orifice and found only a change of a few percent. The increase in pressure drop at the same Reynolds number was larger for water than for silicone oil and glycerin–water solutions, suggesting a possible ionic effect, but there was no difference when salt was added to the water; this suggested no ionic effect. The discrepancy increased as the L/D got bigger (due to the D getting smaller). Their final conclusion was that a new fluid mechanics is needed to explain their data.

Dagan, Weinbaum, and Pfeffer[9] analytically solved the Stokes problem for flow through an orifice with a finite thickness. Their theory shows that the pressure drop depends upon the L/D ratio according to the following formula:

$$\Delta p = \left(\frac{16}{\pi} \frac{L}{D} + 3 \right) \frac{Q\mu}{(D/2)^3}, \tag{3}$$

where Q is the flow rate. This can be rearranged into the form

$$\frac{2\Delta p}{\rho \langle v \rangle^2} = \frac{12\pi}{\mathrm{Re}} + \frac{64}{\mathrm{Re}} \frac{L}{D}. \tag{4}$$

The effect of L/D is to double the pressure drop when L/D is 0.589. The first term is due to Sampson:[12] the analytical solution for an infinitesimally thin orifice at zero Reynolds number (Stokes solution), i.e., for the expansion and contraction. The second term in Eq. (4) is identical to the usual formula for a straight pipe, $f=16/\mathrm{Re}$, i.e., for the length L equal to the thickness of the orifice. While Dagan, Weinbaum, and Pfeffer[9] solved the Stokes problem analytically including a finite thickness of the orifice, their analytical results were correlated within 1% by Eqs. (3) and (4).

Sixty years earlier Bond[10] measured the pressure drop in a flow apparatus that had flow through 0.2–0.29 diameter tubes followed by expansion into a pool of liquid. Combining those results with earlier experiments (Bond[11]) on orifices, he obtained

$$\mu = \frac{\pi R^4 \Delta p}{8Q(L + 2kR)}, \tag{5}$$

where $k=0.573\pm0.009$ and R is the tube radius. This expression can be rearranged into the standard form

$$\frac{2\Delta p}{\rho \langle v \rangle^2} = \frac{1}{\mathrm{Re}} \left(36.7 + 64 \frac{L}{D} \right), \tag{6}$$

which has the identical form as found by Dagan, Weinbaum, and Pfeffer[9] with the constant $12\pi=37.7$ replaced by 36.7. Thus, for Stokes flow, the inclusion of the effect of L/D is well established both theoretically and experimentally.

While Hasegawa, Suganuma, and Watanabe[2] claim that the numerical calculations follow only the bottom curve in Fig. 2 for all L/D, it is clear that the effect of L/D predicted

by Dagan, Weinbaum, and Pfeffer[9] and measured by Bond[10] predicts most of the pressure drop as L/D is increased from 0.092 to 1.14. When Hasegawa, Suganuma, and Watanabe[2] refer to the Dagan paper, they say results of Dagan, Weinbaum, and Pfeffer[9] are closely approximated by Sampson's results,[12] which are not influenced by L/D at all. The appropriate comparison is to Eq. (4) where the effect of L/D is clear.

Johansen[13] measured the orifice coefficient defined as

$$\langle v\rangle = C_o\sqrt{\frac{2\,\Delta p}{\rho[1-(D/D_t)^4]}}, \tag{7}$$

which is the same as

$$\frac{2\,\Delta p}{\rho\langle v\rangle^2} = \frac{1-(D/D_t)^4}{C_o^2}. \tag{8}$$

He found

$$C_o = a\,\mathrm{Re}^{0.5} \tag{9}$$

for Re=0.04–9. This gives

$$\frac{2\,\Delta p}{\rho\langle v\rangle^2} = \frac{1-(D/D_t)^4}{a^2\,\mathrm{Re}} = \frac{K'}{\mathrm{Re}}, \tag{10}$$

where $K'=39.1$, 40.6, and 40.4 (the average is 40.0) for $D/D_t=0.090$, 0.209, and 0.401, respectively, for orifices with a 45° angle. This compares with $K'=12\pi=37.7$ for a sharp-edged orifice. Bond[11] did similar experiments with glycerine–water mixtures passing through orifices and obtained $K'=39.6$ in Eq. (10).

In summary, prior results for Stokes flow and thin orifices are summarized by Eq. (10) with $K'=12\pi=37.7$ (Sampson),[12] 36.7 (Bond),[10] 40.0 (Johansen,[13] 45° orifice), and 39.6 (Bond).[11] When the orifice has significant thickness, the prior results are summarized by Eq. (4) for the theory (Dagan, Weinbaum, and Pfeffer[9]) and Eq. (6) for experiments (Bond[10]). The effect of finite orifice thickness contributes 10% of the pressure drop when $L/D=0.16$, rising to 50% of the total pressure drop when $L/D=0.59$ and 63% when $L/D=1$. Thus, the effect of L/D at low Reynolds number (Re<1) can be predicted with standard continuum mechanics.

III. PRIOR WORK AT LAMINAR INTERMEDIATE REYNOLDS NUMBERS

For higher Reynolds number ($\geqslant$100) the $2\Delta p/\rho\langle v\rangle^2$ approaches an asymptote in Fig. 2. This asymptote has been measured before, too, by Bond[10] (2.23) and Johansen[13] (2.27→2.49 depending on D/D_t). Hasegawa *et al.*[2] obtained a value of 2.17. This value is usually expressed as an orifice coefficient, or $C_o=0.67$ (Bond),[10] 0.63–0.66 (Johansen),[13] and 0.68 (Hasegawa *et al.*).[2] All three authors show the $K=2\Delta p/\rho\langle v\rangle^2$ reaching a minimum at a Reynolds number between 200 and 400 (it is a very shallow minimum), which is the reason C_o reaches a maximum at the same point, as shown in standard handbooks (e.g., Perry and Green[14]).

At Reynolds numbers between the two extremes (1 and 1000), Johansen[13] made careful visual observations. He noticed that for a Reynolds number of 250 (but not for 150) the jet out the orifice had slight vortex ripples and the jet was quite long. For higher Reynolds numbers (600), the vortex ripples are generated closer to the orifice and the flow indicates an incipient instability.

Liu, Afacan, and Masliyah[15] correlated data in orifices for Re from 0 to 10 000. They correlated the data in terms of the friction factor

$$f_d \equiv \frac{\Delta p D}{2\mu\langle v\rangle}. \tag{11}$$

The variable f_d can be related to K, also. Their correlation is

$$K\,\mathrm{Re} = 4f_d = 36 + 64\frac{L}{D} + 1.8\frac{\mathrm{Re}^2}{256+\mathrm{Re}^2}(\mathrm{Re}-8). \tag{12}$$

The correlation fits the experimental data well for Reynolds numbers above 1000, but for Re$\leqslant$1000 the correlation is slightly below the data presented by Liu, Afacan, and Masliyah[15] for the orifice, although it is in good agreement with Kiljanski's data[16] for a free jet. The free jet is not an orifice, though, so that when comparing Liu's correlation to experimental data for orifices, we expect the correlation to be below the data for the Reynolds number range we are considering. The comparison of Liu's correlation and data of Hasegawa, Suganuma, and Watanabe is shown in Fig. 3. As expected, Liu's correlation based mainly on free jet data is slightly below the data of Hasegawa, Suganuma, and Watanabe. At Re=1000, the asymptote is $K=1.83-1.89$ depending on L/D, not a very big difference.

Thus, for intermediate Reynolds numbers, the effect of L/D is small ($K=2.17-2.49$ at Re=1000). It is of interest, though, to calculate the exact experimental cases described by Hasegawa, Suganuma, and Watanabe[2] to see if the data can be predicted, and, if not, which cases show the most discrepancy.

IV. DESCRIPTION OF THE NUMERICAL METHOD

The finite element method was used to solve the incompressible, constant viscosity version of the Navier–Stokes equation for flow through an orifice with finite thickness in a capillary. The program used was FEMLAB, from Comsol. The usual geometry was in a capillary whose diameter was three times the diameter of the orifice with a length 8 or 16 diameters long, with the orifice three to four diameters downstream from the inlet, where the velocity was fully developed flow in a capillary. The calculations were done using an axisymmetric geometry, thus covering only one-half of the domain shown in Fig. 1. Since the diameter of the capillary for the experiments was not given, simulations were done with different capillary diameters to ensure that the chosen diameter was large enough that it had no effect. Table I gives the results, which verify that choice, and all simulations reported here are for a capillary diameter three times the orifice diameter. For Reynolds numbers less than 10, the domain was taken as eight times the orifice diameter, and the answers for pressure drop were within 1% of those calculated on longer domains. That mesh used ≈1500 nodes, 2800 elements, and 13 000 degrees of freedom, and it was refined

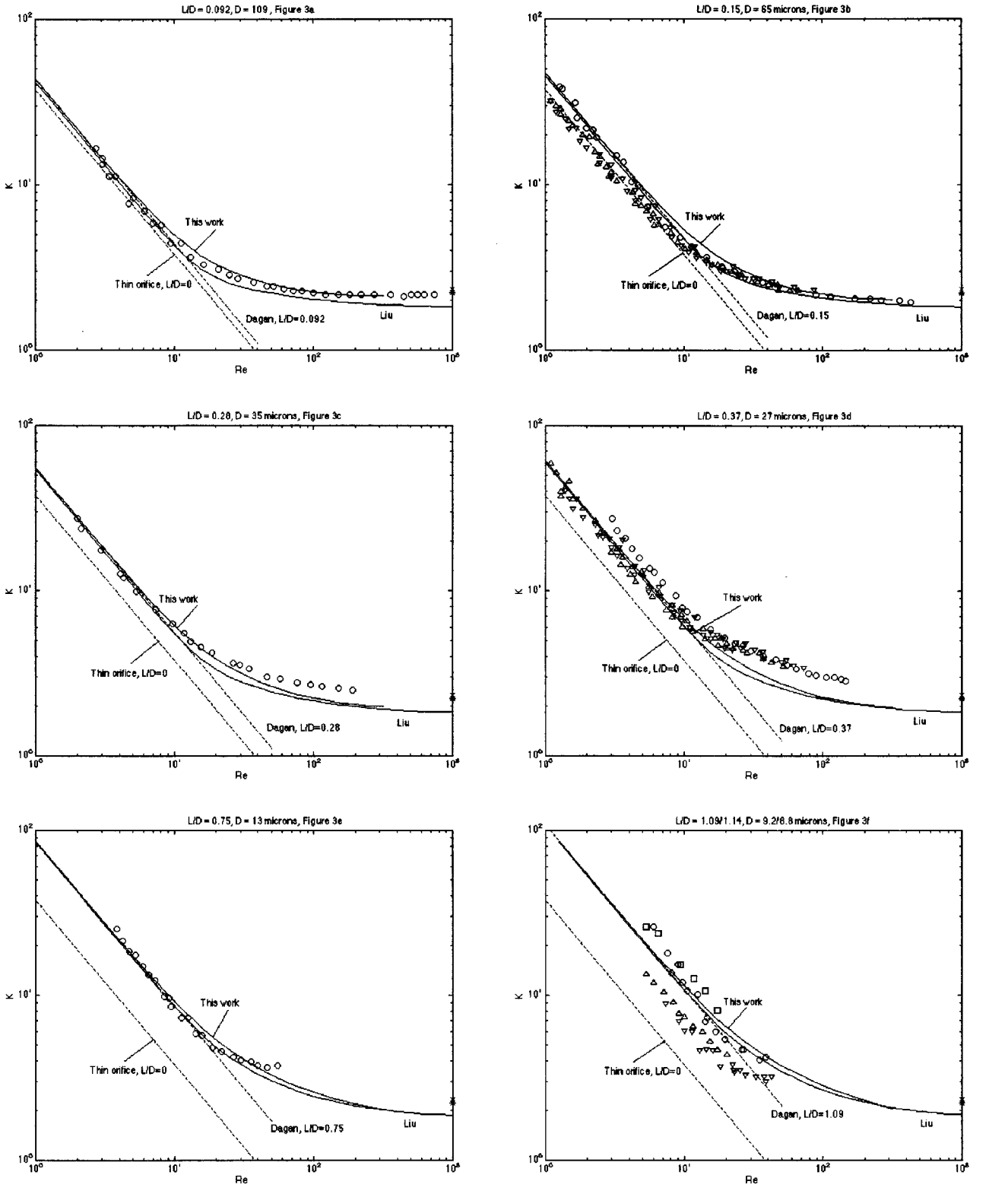

FIG. 3. Pressure coefficient, Eq. (1), as a function of Reynolds number. The dotted lines are the analytical solutions to Stokes flow for specific L/D [Dagan, Weinbaum, and Pfeffer (Ref. 9)] and for $L/D=0$ [Sampson (Ref. 12)]. The solid lines labeled "Liu" are Eq. (12), and the other solid lines are the finite element results. The points at Re=1000 are the asymptotes measured by Bond (*) (Ref. 10) and Johansen (X) (Ref. 13). Points are experimental data of Hasegawa, Suganuma, and Watanabe (Ref. 2) with distilled water (circle and box), glycerin–water solutions (up triangle), and silicone oil (down triangle). Graphs are for (a) $L/D=0.092$, $D=109$ μm, (b) $L/D=0.15$, $D=65$ μm, (c) $L/D=0.28$, $D=35$ μm, (d) $L/D=0.37$, $D=27$ μm, (e) $L/D=0.75$, $D=13$ μm, (f) $L/D=1.09$, $D=9.2$ μm, nickel steel, and $L/D=1.14$, $D=8.8$ μm, Harver steel.

locally around the orifice. For Reynolds numbers between 10 and 316, the length needed to be extended to 16 times the orifice diameter (which gave a pressure drop 3% lower than found on the shorter domain). That mesh used ≈3100 nodes, 6000 elements, and 28 000 degrees of freedom. For Reynolds numbers higher than 316, the length was 32 times the orifice diameter, but it was difficult to have both a refined mesh near the orifice and the longer domain due to memory

TABLE I. Effect of capillary diameter, Re=10, L/D=0.37.

D_t/D	$\Delta p'$	% difference from last entry
2	33.88	0.59
3	34.07	0.03
4	34.08	...

limitations. Thus, no solutions are given here for Reynolds numbers above 316, although they generally showed the same trends as correlation of Liu, Afacan, and Masliyah.[15] Calculations with different meshes gave answers within 1% of each other for Reynolds numbers less than 10 and within 2%–3% of each other for a Reynolds number of 100. The calculations reported are for the most refined mesh, and the percentage difference between the reported results and an extrapolated exact solution would be smaller than these percentages. Differences of this magnitude are not discernable on the figures.

The inlet boundary condition was fully developed flow in a tube, the velocity was zero on all solid surfaces, the centerline employed a symmetry condition, and the exit boundary condition was for no applied external forces; i.e., it used natural boundary conditions in the finite element method. As the Reynolds number increased, it was found that the flow was not fully developed at the exit, but the use of natural boundary conditions permitted solution by the finite element method. This phenomenon agrees with the experimental observations by Johansen.[13]

The equation solved was the traditional Navier–Stokes equation, in nondimensional form,

$$\mathbf{u}' \cdot \nabla' \mathbf{u}' = -\nabla' p' + \frac{1}{\mathrm{Re}} \nabla'^2 \mathbf{u}', \tag{13}$$

where $p' = p/\rho\langle v \rangle^2$, and the dimensionless pressure drop is one-half the pressure coefficient, Eq. (1),

$$\frac{K}{2} = \Delta p'. \tag{14}$$

V. NUMERICAL RESULTS

Figure 3 shows that the finite element results reasonably agree with the experimental data of Hasegawa, Suganuma, and Watanabe,[2] Bond,[10] and Liu, Afacan, and Masliyah.[15] The numerical results either go through the middle of the data of Hasegawa, Suganuma, and Watanabe [Figs. 3(a), 3(b), 3(e), and 3(f)] or are between the data of Hasegawa, Suganuma, and Watanabe and the data of Liu, Afacan, and Masliyah [Figs. 3(c) and 3(d)]. The line for L/D=0 is shown in all figures, and it is clear that L/D is a significant variable. Experimental data for $L/D \geqslant 0.15$ should not be compared with the theory or numerical results made with L/D=0.

Next, consider the data for water only (circles in Fig. 3) and examine Figs. 3(a)–3(f) in turn, representing increasing L/D and decreasing D. The numerical results match the data for Figs. 3(a) and 3(b) extremely well. In Fig. 3(c), the numerical results match the data up until about Re=20, and then the numerical results are below the data. In Fig. 3(d) the water data are everywhere above the calculations, but agreement is recovered in Fig. 3(e). In Fig. 3(f) the data are above and below the numerical results.

Finally, consider Figs. 3(b), 3(d), and 3(f) and look at the data for glycerin–water solutions and silicone oil. The experimental data for these fluids are always below the experimental data for water. The experimental data for these fluids are below the numerical calculations in Figs. 3(b) and 3(f), but agree with the numerical results in Fig. 3(d). Thus, the experimental data give a contradictory picture.

There are two additional possible complications. The first is that the shear rates are extremely high in such micrometer devices. While the peak shear rates in the orifice flow are no more than two to three times those achieved in fully developed flow, in 10–100 μm sized devices those shear rates are huge ($\leqslant 10\,000\ \mathrm{s}^{-1}$) at the highest Re for which data were taken in each L/D. It is possible that the viscosity is not Newtonian under those conditions, and that this effect is greater for water than for glycerin–water solutions and silicone oil. The second feature is the possibility of viscous dissipation causing an increase in temperature. Estimates of this effect indicate that the temperature rise is less than 1 °C, so that this is not important.

While there are some unexplained discrepancies between the numerical calculations and the experimental data, those discrepancies follow no trend. Thus, we conclude that the experimental data are mostly explained by standard continuum theory provided the effect of L/D is included.

VI. CONCLUSIONS

Standard continuum mechanics for an incompressible Newtonian fluid is shown to explain most of the data for pressure drop through an orifice as measured by Hasegawa, Suganuma, and Watanabe[2] in small devices (diameter < 100 μm). The simulations cover Reynolds numbers from 1 to 316, and L/D from 0.092 to 1.14 when the orifice diameter is as small as 8.8 μm. For small diameters, the data for water are considerably above the theory for L/D=0, but the data are only slightly above the more applicable theory due to Dagan, Weinbaum, and Pfeffer[9] (Re=0 and various L/D) or the calculations presented here for nonzero L/D and $1 \leqslant \mathrm{Re} \leqslant 300$. For the smallest diameters, the data for glycerin solutions and silicone oil are below both the water data and the numerical results. In summary, for most of the cases there is no need to invent a new fluid mechanics to explain these data.

ACKNOWLEDGMENT

The authors would like to thank Professor Daniel T. Schwartz, University of Washington, for helpful comments.

[1]C.-M. Ho and Y.-C. Tai, "Micro-electric-mechanical-systems (MEMS) and fluid flow," Annu. Rev. Fluid Mech. **30**, 579 (1998).
[2]T. Hasegawa, M. Suganuma, and H. Watanabe, "Anomaly of excess pressure drops of the flow through very small orifices," Phys. Fluids **9**, 1 (1997).
[3]A. J. Gijsbertsen-Abrahamse, A. van der Padt, and R. M. Boom, "Influence of membrane morphology on pore activation in membrane emulsification," J. Membr. Sci. **217**, 141 (2003).
[4]T. K. Hsiai, S. K. Gho, J. M. Yang, X. Yang, Y. C. Tai, and C.-M. Ho, "Pressure drops of water flow through micromachines particle filters," J. Fluids Eng. **124**, 1053 (2003).
[5]G. G. A. Janssens-Maenhout and T. Schulenberg, "An alternative description of the interfacial energy of a liquid in contact with a solid," J. Colloid Interface Sci. **257**, 141 (2003).
[6]D. Yao and B. Kim, "Simulation of the filling process in microchannels for polymeric materials," J. Micromech. Microeng. **12**, 604 (2002).
[7]X. Y. Chen, K. C. Toh, C. Yang, and J. C. Chai, "Numerical computation of hydrodynamically and thermally developing liquid flow in microchannels with electrokinetics effects," ASME Trans. J. Heat Transfer **126**, 70 (2004).
[8]X. Y. Chen, K. C. Toh, J. C. Chai, and C. Yang, "Developing pressure-driven liquid flow in microchannels under the electrokinetic effect," Int. J. Eng. Sci. **42**, 609 (2004).
[9]Z. Dagan, S. Weinbaum, and R. Pfeffer, "An infinite-series solution for the creeping motion through an orifice of finite length," J. Fluid Mech. **115**, 505 (1982).
[10]W. N. Bond, "The effect of viscosity on orifice flows," Proc. Phys. Soc. London **34**, 139 (1922).
[11]W. N. Bond, "Viscosity determination by means of orifices and short tubes," Proc. Phys. Soc. London **33**, 225 (1921).
[12]R. A. Sampson, "On Stokes's current function," Philos. Trans. R. Soc. London, Ser. A **182**, 449 (1891).
[13]F. C. Johansen, "Flow through pipe orifices at low Reynolds numbers," Proc. R. Soc. London, Ser. A **126**, 231 (1930).
[14]R. H. Perry and D. W. Green, *Perry's Chemical Engineers' Handbook*, 7th ed. (McGraw-Hill, New York, 1997), pp. 10–16.
[15]S. Liu, A. Afacan, and J. H. Masliyah, "A new pressure drop model for flow-through orifice plates," Can. J. Chem. Eng. **79**, 100 (2001).
[16]T. Kiljanski, "Discharge coefficient for free jets from orifices at low Reynolds number," J. Fluids Eng. **115**, 778 (1993).